THE JOURNAL OF PHYSICAL CHEMISTRY Letters

Letter

Cite This: J. Phys. Chem. Lett. 2018, 9, 5877−5883

pubs.acs.org/JPCL

Fundamental Link between β Relaxation, Excess Wings, and Cage-Breaking in Metallic Glasses

Hai-Bin Yu,[*,†] Meng-Hao Yang,[*,‡,§] Yang Sun,[‡] Feng Zhang,[‡] Jian-Bo Liu,[§] C. Z. Wang,[‡,∥] K. M. Ho,[‡,∥] Ranko Richert,[⊥] and Konrad Samwer[#]

[†]Wuhan National High Magnetic Field Center and School of Physics, Huazhong University of Science and Technology, WuHan, Hubei 430074, China

[‡]Ames Laboratory, U.S. Department of Energy, Ames, Iowa 50011, United States

[§]Key Laboratory of Advanced Materials (MOE), School of Materials Science and Engineering, Tsinghua University, Beijing 100084, China

[∥]Department of Physics, Iowa State University, Ames, Iowa 50011, United States

[⊥]School of Molecular Sciences, Arizona State University, Tempe, Arizona 85287, United States

[#]I. Physikalisches Institut, Universität Göttingen, D-37077 Göttingen, Germany

ABSTRACT: In glassy materials, the Johari−Goldstein secondary (β) relaxation is crucial to many properties as it is directly related to local atomic motions. However, a long-standing puzzle remains elusive: why some glasses exhibit β relaxations as pronounced peaks while others present as unobvious excess wings? Using microsecond atomistic simulation of two model metallic glasses (MGs), we demonstrate that such a difference is associated with the number of string-like collective atomic jumps. Relative to that of excess wings, we find that MGs having pronounced β relaxations contain larger numbers of such jumps. Structurally, they are promoted by the higher tendency of cage-breaking events of their neighbors. Our results provide atomistic insights for different signatures of the β relaxation that could be helpful for understanding the low-temperature dynamics and properties of MGs.

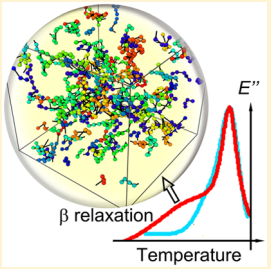

If a liquid is cooled to temperatures below its melting point, it forms either a crystalline solid or a metastable supercooled liquid with sluggish dynamics. In the latter case, the structural (α) relaxation time increases enormously upon cooling and eventually reaches values typical for solid materials at the glass transition temperature.[1] As the α relaxation time becomes so long that it appears as frozen in the glassy states, an additional process called the Johari−Goldstein secondary (β) relaxation becomes the principal source of dynamics in the glassy state.[2−6] It is related to local atomic motions in an otherwise rigid glass and hence of significance to the understanding of several crucial unresolved issues in glassy physics and material sciences[7−10] (and see, e.g., refs 1 and 11−14 for reviews). We note that there are some other processes also called secondary relaxation, but we follow the work of Ngai et al.[3,6] to use the name "Johari−Goldstein β relaxation" to indicate that they are sensitive to intermolecular interactions and not to intramolecular degrees of freedom.

One intriguing feature about β relaxation has attracted considerable attention in the glass community. In some glass formers, the β relaxations manifest as distinct peaks as probed by mechanical or dielectric loss spectra, while in some other glasses, the β relaxations appear to be absent and, instead, excess contributions to the tails of α relaxations show up, which are the so-called excess wings.[15−19] Notably, the behaviors of β relaxations are sensitive to chemical compositions and processing histories.[17,18,20−28] There are a few empirical rules or correlations,[3,17,21,22] and especially the coupling model[1,3,6] can rationalize the relationship between β relaxations and some other properties. Nevertheless, it is still not easy to predict which glasses would show pronounced β relaxations or excess wings from the first principle; it represents a challenging issue in glassy physics.[29−36] Meanwhile, the presence of β relaxations (or excess wings) is related to a number of important properties of glassy materials, ranging from mechanical ductility of metallic and polymeric glasses[1,37−40] to stability of glassy medicines.[19,41] As a result, a mechanistic understanding of the distinctions between pronounced β relaxations and excess wings could have broad implications.[1,10,11,42,43]

As indicated by experiments, β relaxations separate from the primary (α) processes upon cooling only after structural dynamics become slower than about 1 μs. Thus, in order to disentangle the β relaxation from α relaxation in simulations, the observation time must be on the order of microseconds or more.[2,4]

Recently, the structural mechanism governing the β relaxations has been investigated in a model metallic glass (MG) by mircosecond atomistic simulations,[29] which show that string-like motions might be the origin of β relaxation in

Received: August 25, 2018
Accepted: September 21, 2018
Published: September 21, 2018

DOI: 10.1021/acs.jpclett.8b02629
J. Phys. Chem. Lett. 2018, 9, 5877−5883

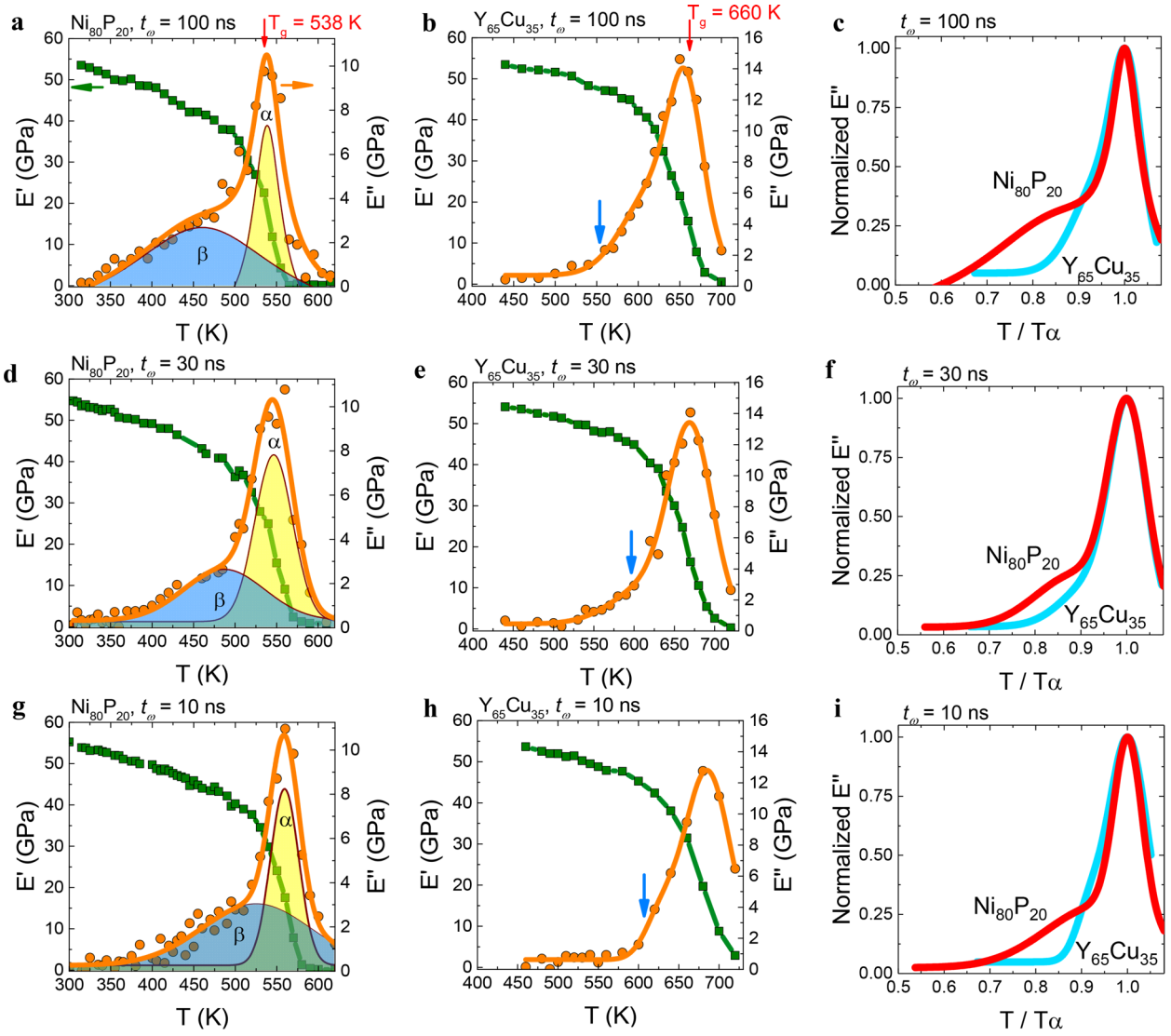

Figure 1. Probing β relaxation and excess wings in MGs. The storage (E') and loss (E'') moduli of the $Ni_{80}P_{20}$ model MG (a,d,g; i.e., the first column, data taken from ref 29) and the $Y_{65}Cu_{35}$ model MG (b,e,h; i.e., the second column) at different testing periodic t_ω values, as indicated. (c,f,i; i.e.; the third column). Comparisons of normalized E'' as a function of scaled temperature at different values of t_ω. The blue and yellow shaded areas are two functions to fit the global E'' of $Ni_{80}P_{20}$; however, for $Y_{65}Cu_{35}$, the fittings are elusive and thus not conducted. The blue arrows in the middle column indicate the temperature that E'' most likely deviates from for a single-peak profile. The red arrows in (a) and (b) indicate the glass transition temperature (T_g) independently determined from the volume−temperature relation during cooling.

MGs. Also note that string-like motions have been studies in several other models.[44−48] In this connection, it could be revealing to study whether and how this mechansim can rationalize the distiction between pronounced β relaxation and excess wings in different MGs.

Figure 1 shows the storage (E') and loss moduli (E'') of the two systems determined from MD simulations of dynamical mechanical spectroscopy (MD-DMS; see the Simulation Methods section). The first and second columns are the results for $Ni_{80}P_{20}$ and $Y_{65}Cu_{35}$ model MGs, respectively. Our main motivation for choosing these two models is that the atomic radii ratios for them are very similar; therefore, the interatomic interaction strength could be responsible for the difference in dynamics.

As a typical example, Figure 1a shows the E' (left axis) and E'' (right axis) as a function of temperature at a fixed oscillation period, t_ω = 100 ns (related with frequency $f = 1/t_\omega$) for the $Ni_{80}P_{20}$ MG.[29] Besides the dominant α relaxation (the rapid drop of E' or the peak of E'' at $T \approx 550$ K), there is an additional peak in E'' at lower temperature, which can be assigned to the Johari−Goldstein β relaxation.[29] Figure 1b shows similar data for the $Y_{65}Cu_{35}$ MG, but it is difficult to identify a distinct β relaxation peak given that the α relaxation dominates the E'' curve. Only an excess contribution to the left flank of α relaxation might be discerned, that is, the excess wing. Figure 1c compares E'' for these two model MGs in a normalized plot where E'' and T are scaled by the maximum value of E'' and its temperature. We find that the $Ni_{80}P_{20}$ MG has a pronounced β relaxation, whereas only an excess wing appears for the $Y_{65}Cu_{35}$ case. A similar feature has been observed in two other different values of t_ω = 30 (Figure 1d−f) and 10 ns (Figure 1g−i). The contrasting behaviors of the two model MGs provide an opportunity to elucidate their structural origins by MD simulations.

Figure 2a,b compares two atomic configurations at T = 455 K for $Ni_{80}P_{20}$ and T = 560 K for $Y_{65}Cu_{35}$, respectively. The

DOI: 10.1021/acs.jpclett.8b02629
J. Phys. Chem. Lett. 2018, 9, 5877−5883

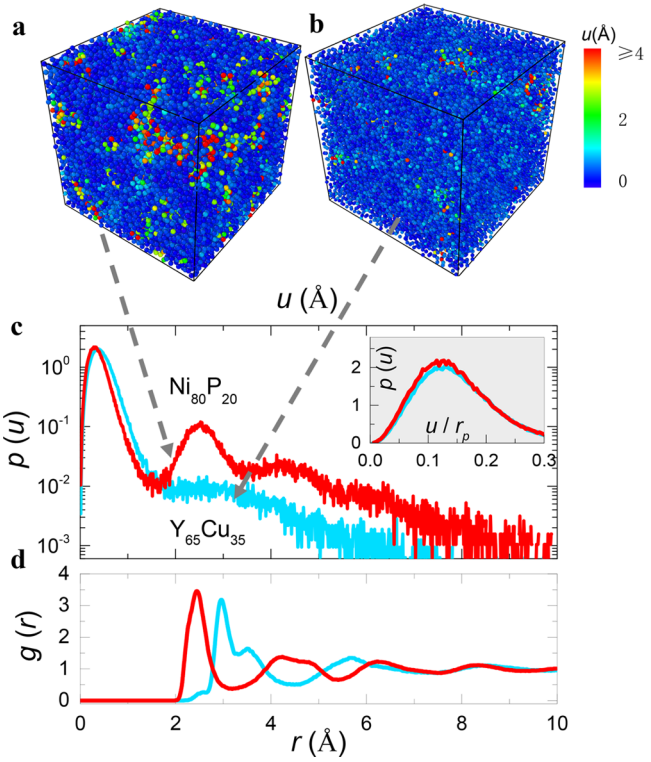

Figure 2. Atomic displacements corresponding to β relaxation and excess wings in MGs. Atomic configurations for (a) T = 455 K for $Ni_{80}P_{20}$ and (b) T = 560 K for $Y_{65}Cu_{35}$. Both temperatures are at $0.85T_\alpha$ (t_ω = 100 ns) for the two MGs. The color codes represent atomic displacements u over 100 ns. (c) Statistics $p(u)$ of u for the two model MGs. (d) Radial distribution function $g(r)$ of the model MGs; all of the atoms are selected in determining $g(r)$. The inset of (c) is $p(u)$ versus u/r_p, where r_p is first peak position of $g(r)$.

temperatures are selected based on $0.85T_\alpha$ (t_ω = 100 ns) (here, T_α is the peak temperature in Figure 1a,b), where the β relaxation is most prominent for $Ni_{80}P_{20}$ and where the excess wing onset appears for $Y_{65}Cu_{35}$ (see Figure1c). The color codes represents the atomic displacement magnitude u for every atom defined as $u_i(t) = |\vec{r}_i(t) - \vec{r}_i(0)|$ over a waiting time t = 100 ns. Heterogeneous dynamics are observed in both configurations, as can be directly seen in Figure 2a,b. Compared to $Y_{65}Cu_{35}$ (Figure 2b), the $Ni_{80}P_{20}$ MG (Figure 2a) contains more atoms with larger u. Figure 2c quantifies their difference by showing the probability density function[49] $p(u)$ based on the statistics of u. Consistent with the images of Figure 2a,b, $Ni_{80}P_{20}$ has a greater fraction of large u than $Y_{65}Cu_{35}$. We also note that $Ni_{80}P_{20}$ has three discernible peaks separated by two valleys on $p(u)$, whereas there is only one peak and a hump for $Y_{65}Cu_{35}$. Figure 2d shows the pair distribution function $g(r)$ of the MGs, which relates to the probability of finding an atom at a distance r away from a reference atom. Specific for $Ni_{80}P_{20}$, one can see that the positions of first and second peaks of $g(r)$ match exactly the second and third peaks of $p(u)$. This implies that atoms with large values of u rearrange by cooperative jumps: one atom jumps to the position that is previously taken by another atom in its nearest or secondary neighbors. In other words, the jumps are from shell to shell. Similar signatures also hold for $Y_{65}Cu_{35}$, although less obvious (by about a factor of 10).

Figure 3a,b shows the displacement vectors at the same temperature and waiting time as Figure 2. For clarity, the two-dimension (2D) slices with a thickness of 1 nm are displayed. We define displacement larger than u_c = 1.8 Å [corresponding to the first minimum in $p(u)$ in Figure 2c] as fast-moving atoms, and they are indicated by red color; blue represents the slow-moving atoms. We find that many of the fast-moving atoms form string-like configurations. Figure 3c,d highlights the 3D string-like motions for the two MGs; other atoms that are not involved in the strings are removed for a clear view. One can see that $Ni_{80}P_{20}$ has more string-like configurations than $Y_{65}Cu_{35}$, and most of the strings in the $Ni_{80}P_{20}$ MG are longer than that of $Y_{65}Cu_{35}$. Such differences are supported by Figure 3e,f, which present the distribution of the number of atoms in a string n_{str} for the two MGs. For example, the longest strings in $Ni_{80}P_{20}$ contain about 10 atoms, while there are 4 atoms for that of $Y_{65}Cu_{35}$. Generally, the population decreases with n_{str} and might be tentatively fitted by a function of exponential decay.

Figure 4a,b shows the time evolutions of N_{str}/N_{fast}, the fraction of the number of atoms in string-like jumps to the number of fast-moving atoms as a function of time for different temperatures for the two model MGs. At each temperature, the values of N_{str}/N_{fast} first increase with time but then decrease at longer times, exhibiting a finite maximum at a specific time, defined as τ_{str}. Physically, τ_{str} measures the most probable time for the observation of the string-like motions in the background of fast-moving atoms. At the same time, the height of the peak [i.e., $N_{str}/N_{fast}(\tau_{str})$] grows with lowering temperatures, which indicates the increasing degree of cooperativity. Although both MGs follow similar general trends, they have a marked difference in the attainable values of $N_{str}/N_{fast}(\tau_{str})$. For instance, the $Ni_{80}P_{20}$ MG contains as much as twice the string-like motions as the $Y_{65}Cu_{35}$ MG at the same scaled temperature.

Figure 4c recast the data of Figure 4a for $Ni_{80}P_{20}$ in terms of a 2D contour plot where the values N_{str}/N_{fast} are represented by color codes. The temperature and time of the β relaxation as decomposed from Figure 1a,d,g are shown as discrete stars. We find that a remarkable match between the β relaxation and the ridge of N_{str}/N_{fast}, as shown by the dashed line. This suggest that the β relaxation occurs when most of the fast-moving atoms are string-like, implying that the string-like motions could be the mechanism of β relaxation in this $Ni_{80}P_{20}$ MG. Figure 4d reports similar findings in the $Y_{65}Cu_{35}$ MG. Because it has excess wings instead of pronounced peaks, the determination of β relaxation is less accurate than that of $Ni_{80}P_{20}$, and we thus use the temperature as indicated by the arrows in Figure 1b,e,h, where the deviations from the tails of α relaxation are evident. We see that the excess wing is correlated with the ridge of N_{str}/N_{fast} for this MG as well.

The above findings suggest that both the β relaxation and the excess wing have the same origin from the string-like cooperative jumps; their distinctions are from the different amounts of these jumps. They are also reminiscent of an "islands of mobility" scenario, as previously suggested.[2,50] However, we see this in a short time frame; it does not imply long-time persistence of that pattern.

Why do the two model MGs have different amounts of string-like motions that influence the behaviors of β relaxations? We consider the caging properties of a precursor for them. In glassy states, most of the atoms are confined in transient cages formed by their neighbors. This prevents them from diffusing freely throughout the sample. Intuitively, to form string-like motions, the atoms must first escape from their

DOI: 10.1021/acs.jpclett.8b02629
J. Phys. Chem. Lett. 2018, 9, 5877−5883

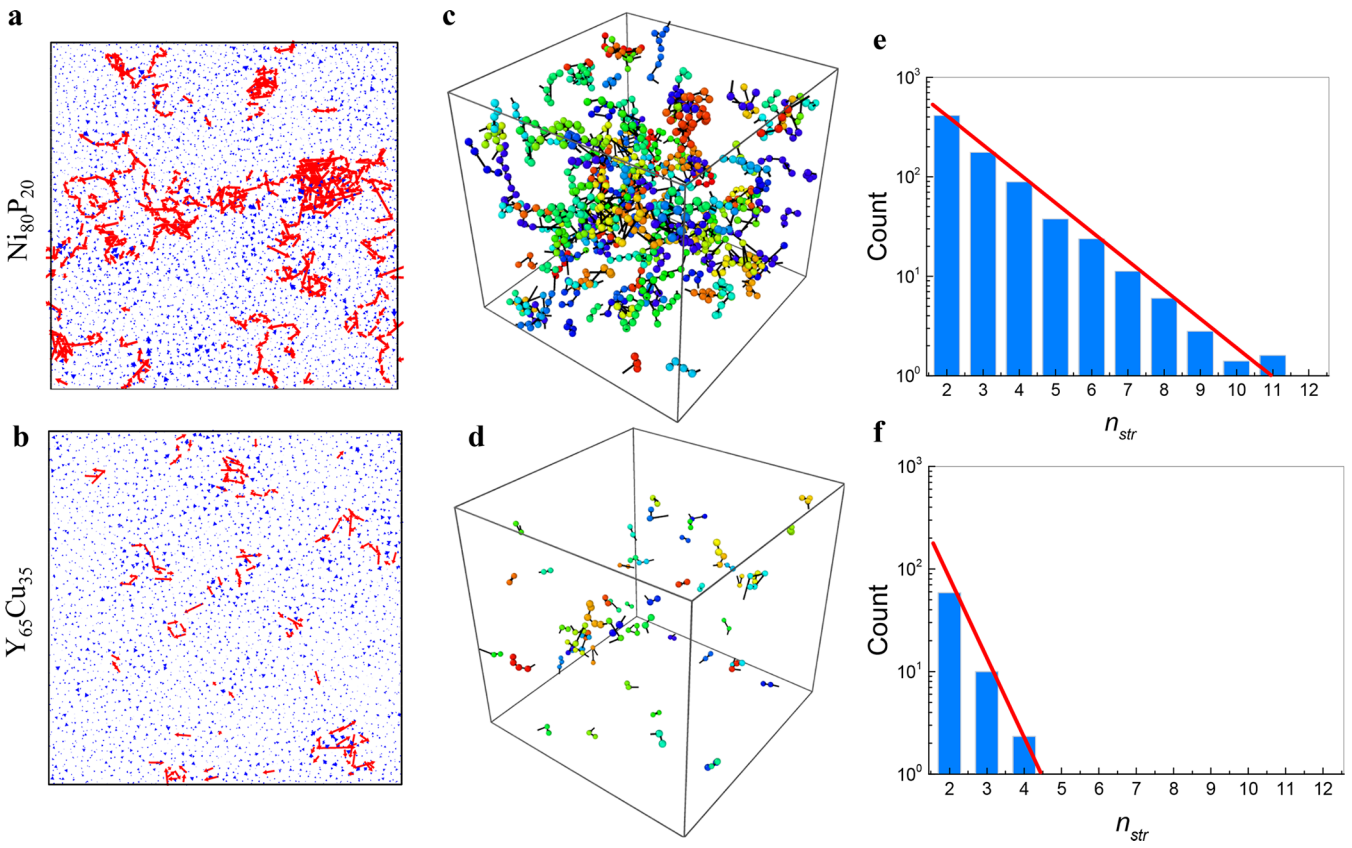

Figure 3. String-like cooperative atomic jumps in MGs. Atomic displacement vectors for (a) $Ni_{80}P_{20}$ and (b) $Y_{65}Cu_{35}$ MGs; the slice is 1 nm. String-like atomic displacements for (c) $Ni_{80}P_{20}$ and (d) $Y_{65}Cu_{35}$ MGs. Statistics of the number of atoms in string-like motions (N_{str}) for (e) $Ni_{80}P_{20}$ and (f) $Y_{65}Cu_{35}$ MGs. The red smooth curves in (e) and (f) are fitted by an exponential decay function.

cages. One can thus anticipate that the caging properties could influence the string-like jumps and the β relaxations as a consequence.[42,51−53]

As schematically shown in Figure 4e, we define the number of atoms that break the cage as the cage-breaking fraction $C(T,t = \delta t) \equiv N_{lost}/N_{nb}$ at a temperature T and over a time δt, where N_{nb} is the number of atoms that are the nearest neighbors of one reference atom at $t = 0$; N_{lost} is the number of atoms that are no longer the nearest neighbors at $t = \delta t$ but that were previously the nearest neighbors at $t = 0$. We use the Voronoii tessellation method to identify the nearest neighbors.

Figure 4f shows $C(T,t)$ as a function of waiting time t at the same scaled temperature $T = 0.85T_\alpha$ (t_ω = 100 ns) for $Ni_{80}P_{20}$ (T = 455 K) and $Y_{65}Cu_{35}$ (T = 560 K), respectively. We find that at short time t < 1 ns the values of $C(t)$ are low for both MGs. However, a considerable difference between them develops for longer t and, notably, $C(t)$; the $Ni_{80}P_{20}$ MG increases more rapidly than that of $Y_{65}Cu_{35}$. Particularly, for t = 100 ns (which is the time scale of the β relaxation as well as the most probable time of string-like motions at the considered temperature), $C(t)$ is more than 0.15 for $Ni_{80}P_{20}$, while $C(t)$ = 0.09 for the $Y_{65}Cu_{35}$ MG, indicating that the cages of the $Ni_{80}P_{20}$ MG are more prone to break. Additional information can be gained from Figure 4g, which reports $C(T,t = \delta t)$ as a function of temperature scaled by T_α (t_ω = 100 ns) for a fixed δt = 100 ns for the two MGs; their difference is evident in the temperature range relevant for the β relaxations.

Recently, the connections between β relaxations and the caging properties in different glasses[42,51−53] have been discussed based on the coupling model. Our findings provide a direct atomistic picture. We may attribute the excess wings to be less developed β relaxations as the atoms start to break the cage quite late and cannot develop the string-like motions because structural α-relaxation arises soon, bringing cage collapse and global diffusions.

In summary, by atomistic simulations of two model MGs up to the time scale of microseconds, we offer a structural basis for the difference between the pronounced β relaxations and excess wings in MGs. The emerging physical picture is that string-like cooperative atomic jumps are directly correlated to both the β relaxation and the excess wing, and thus, they have the same origin regarding the cage-breaking process, which might depend on the interatomic potentials.[21,54] Their distinctive behavior stems from the richness of these string-like motions, which is linked to the cage-breaking tendency as a precursor. Future studies should address how local properties impact cage-breaking and whether this concept applies to other classes of glass formers. Some previous simulations indicated that string-like motions might be abundant in some atomic[44,47] and polymeric models[48] but scarce in a covalent model;[55] it would be interesting to see whether they are correlated to the Johari−Goldstein β relaxation as well.

SIMULATION METHODS

We used the LAMMPS software to conduct MD simulations. Our model system contains N = 32000 atoms. Two model systems, namely, $Ni_{80}P_{20}$ and $Y_{65}Cu_{35}$, were studied. They interacted with an embedded atom method potential from Sheng et al.[56,57] and Wang et al.,[58] respectively. Some of the data (i.e., Figures 1a, 1d, 1g, and 2a) of the $Ni_{80}P_{20}$ have been

DOI: 10.1021/acs.jpclett.8b02629
J. Phys. Chem. Lett. 2018, 9, 5877−5883

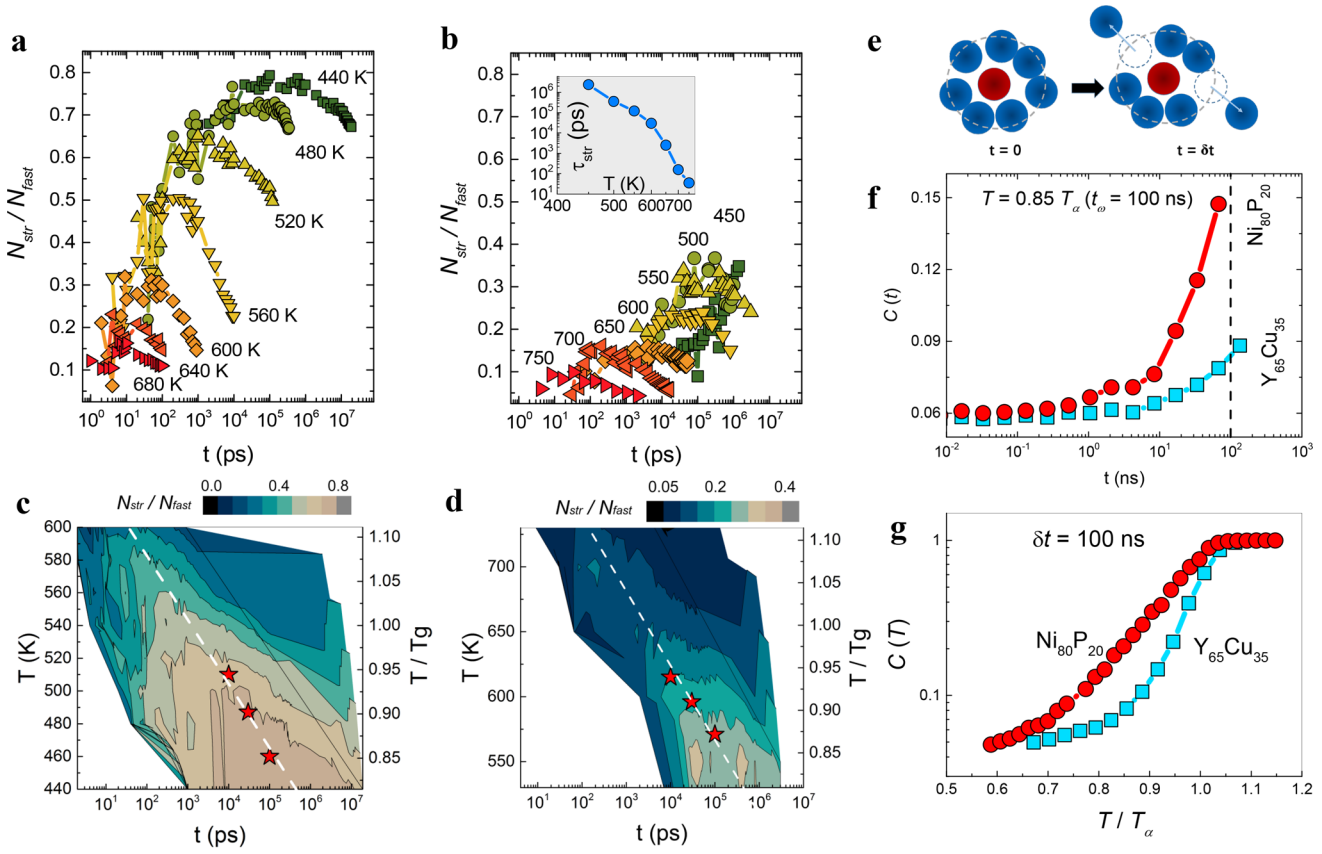

Figure 4. Relationship between string-like motions and cage-breaking and β relaxation. The fraction of atoms in string-like configurations to the total number of fast-moving atoms (N_{str}/N_{fast}) as a function of time for different temperatures for (a) $Ni_{80}P_{20}$ (data taken from ref 29) and (b) $Y_{65}Cu_{35}$ MGs. The inset of (b) is the peak position τ_{str} as a function of temperature. 2D contour plots of N_{str}/N_{fast} are shown in (c) $Ni_{80}P_{20}$ and (d) $Y_{65}Cu_{35}$, respectively. (e) Schematic for the definition of cage-breaking. Cage-breaking fraction $C(T,t)$ for the two MGs (f) as a function of time t for a fixed scaled temperature of $0.85T_\alpha$ and (g) as a function scaled temperature for a fixed time t = 100 ns.

published,[29] but they are included (and replotted) for the purpose of a contrast between the two models. The samples were prepared by quenching a liquid from 1000 to 200 K at a rate of 0.1 K/ns. We used *NPT* ensembles during the quenching. The external pressure was adjusted to around zero. Periodic boundary conditions were applied for all of the simulations.

Dynamics of β relaxations were studied by an approach of MD simulations of dynamical mechanical spectroscopy (MD-DMS)[59,60] that numerically reproduces the protocol of real DMS experiments.[11,12] Specifically, at a temperature T, we apply a sinusoidal strain $\varepsilon(t) = \varepsilon_A \sin(2\pi t/t_\omega)$ with a period t_ω(related to frequency $f = 1/t_\omega$) and a strain amplitude ε_A along the x direction of the model MG, and the resulting stress $\sigma(t)$ and the phase difference between the stress and strain δ are measured and fitted with $\sigma(t) = \sigma_0 + \sigma_A \sin(2\pi t/t_\omega + \delta)$. From these values, storage (E') and loss (E'') moduli are calculated according to $E' = \sigma_A \sin \delta/\varepsilon_A$ and $E'' = \sigma_A \cos \delta/\varepsilon_A$, respectively. We use strain amplitude ε_A = 0.71% for all MD-DMS, which ensures that the deformation is in the linear response regime and E' and E'' are independent of ε_A within resolution.

AUTHOR INFORMATION

Corresponding Authors

*E-mail: haibinyu@hust.edu.cn (H.-B.Y.).
*E-mail: myang@ameslab.gov (M.-H.Y).

ORCID

Hai-Bin Yu: 0000-0003-0645-0187
Meng-Hao Yang: 0000-0002-4791-354X
Yang Sun: 0000-0002-4344-2920
Jian-Bo Liu: 0000-0001-6516-6966
C. Z. Wang: 0000-0002-0269-4785
Ranko Richert: 0000-0001-8503-3175

Notes

The authors declare no competing financial interest.

ACKNOWLEDGMENTS

The computational work was carried out at the TianHe-1(A) of the National Supercomputer Center in Tianjin, China and the TianHe-2 of the National Supercomputer Center in Guangzhou, China and the Gesellschaft fur wissenschaftliche Datenverarbeitung, Göttingen (GWDG), Germany. H.-B.Y. acknowledges support from the National Science Foundation of China (NSFC 51601064) and the National Thousand Young Talents Program of China. K.S. acknowledges support from the German Science Foundation within the FOR 1394, P1. Work conducted at Ames Laboratory was supported by the U.S. Department of Energy, Basic Energy Sciences, Materials Science and Engineering Division, under Contract No. DE-AC02-07CH11358, including a grant of computer time at the National Energy Research Supercomputing Center (NERSC) in Berkeley, CA.

DOI: 10.1021/acs.jpclett.8b02629
J. Phys. Chem. Lett. 2018, 9, 5877−5883

REFERENCES

(1) Ngai, K. L. *Relaxation and Diffusion in Complex Systems*; Springer: New York, 2011.
(2) Johari, G. P.; Goldstein, M. Viscous Liquids and the Glass Transition. II. Secondary Relaxations in Glasses of Rigid Molecules. *J. Chem. Phys.* **1970**, *53*, 2372−2388.
(3) Ngai, K. L.; Paluch, M. Classification of secondary relaxation in glass-formers based on dynamic properties. *J. Chem. Phys.* **2004**, *120*, 857−873.
(4) Kudlik, A.; Tschirwitz, C.; Benkhof, S.; Blochowicz, T.; Rossler, E. Slow secondary relaxation process in supercooled liquids. *Europhys. Lett.* **1997**, *40*, 649−654.
(5) Capaccioli, S.; Paluch, M.; Prevosto, D.; Wang, L.-M.; Ngai, K. L. Many-Body Nature of Relaxation Processes in Glass-Forming Systems. *J. Phys. Chem. Lett.* **2012**, *3*, 735−743.
(6) Ngai, K. L. Relation between some secondary relaxations and the α relaxations in glass-forming materials according to the coupling model. *J. Chem. Phys.* **1998**, *109*, 6982−6994.
(7) Geirhos, K.; Lunkenheimer, P.; Loidl, A. Johari-Goldstein Relaxation Far Below T-g: Experimental Evidence for the Gardner Transition in Structural Glasses? *Phys. Rev. Lett.* **2018**, *120*, 085705.
(8) Olsen, N. B.; Christensen, T.; Dyre, J. C. Time-Temperature Superposition in Viscous Liquids. *Phys. Rev. Lett.* **2001**, *86*, 1271−1274.
(9) Cerveny, S.; Mallamace, F.; Swenson, J.; Vogel, M.; Xu, L. Confined Water as Model of Supercooled Water. *Chem. Rev.* **2016**, *116*, 7608−7625.
(10) Sattig, M.; Vogel, M. Dynamic Crossovers and Stepwise Solidification of Confined Water: A 2H NMR Study. *J. Phys. Chem. Lett.* **2014**, *5*, 174−178.
(11) Yu, H. B.; Wang, W. H.; Bai, H. Y.; Samwer, K. The β-relaxation in metallic glasses. *Natl. Sci. Rev.* **2014**, *1*, 429−461.
(12) Yu, H.-B.; Wang, W.-H.; Samwer, K. The β relaxation in metallic glasses: an overview. *Mater. Today* **2013**, *16*, 183−191.
(13) Wang, W. H. Correlation between relaxations and plastic deformation, and elastic model of flow in metallic glasses and glass-forming liquids. *J. Appl. Phys.* **2011**, *110*, 053521.
(14) Qiao, J. C.; Pelletier, J. M. Dynamic Mechanical Relaxation in Bulk Metallic Glasses: A Review. *J. Mater. Sci. Technol.* **2014**, *30*, 523−545.
(15) Zhao, Z. F.; Wen, P.; Shek, C. H.; Wang, W. H. Measurements of slow beta-relaxations in metallic glasses and supercooled liquids. *Phys. Rev. B* **2007**, *75*, 174201.
(16) Gainaru, C.; Kahlau, R.; Rössler, E. A.; Böhmer, R. Evolution of excess wing and β-process in simple glass formers. *J. Chem. Phys.* **2009**, *131*, 184510.
(17) Doss, A.; Paluch, M.; Sillescu, H.; Hinze, G. From strong to fragile glass formers: Secondary relaxation in polyalcohols. *Phys. Rev. Lett.* **2002**, *88*, 095701.
(18) Schneider, U.; Brand, R.; Lunkenheimer, P.; Loidl, A. Excess wing in the dielectric loss of glass formers: A Johari-Goldstein beta relaxation? *Phys. Rev. Lett.* **2000**, *84*, 5560−5563.
(19) Rösner, P.; Samwer, K.; Lunkenheimer, P. Indications for an ″excess wing″ in metallic glasses from the mechanical loss modulus in Zr 65 Al 7.5 Cu 27.5. *Europhys. Lett.* **2004**, *68*, 226.
(20) Yu, H. B.; Wang, Z.; Wang, W. H.; Bai, H. Y. Relation between β relaxation and fragility in LaCe-based metallic glasses. *J. Non-Cryst. Solids* **2012**, *358*, 869−871.
(21) Yu, H. B.; Samwer, K.; Wang, W. H.; Bai, H. Y. Chemical influence on beta-relaxations and the formation of molecule-like metallic glasses. *Nat. Commun.* **2013**, *4*, 2204.
(22) Zhu, Z. G.; Li, Y. Z.; Wang, Z.; Gao, X. Q.; Wen, P.; Bai, H. Y.; Ngai, K. L.; Wang, W. H. Compositional origin of unusual β-relaxation properties in La-Ni-Al metallic glasses. *J. Chem. Phys.* **2014**, *141*, 084506.
(23) Pronin, A. A.; Kondrin, M. V.; Lyapin, A. G.; Brazhkin, V. V.; Volkov, A. A.; Lunkenheimer, P.; Loidl, A. Glassy dynamics under superhigh pressure. *Phys. Rev. E* **2010**, *81*, 041503.
(24) Yu, H. B.; Tylinski, M.; Guiseppi-Elie, A.; Ediger, M. D.; Richert, R. Suppression of beta Relaxation in Vapor-Deposited Ultrastable Glasses. *Phys. Rev. Lett.* **2015**, *115*, 185501.
(25) Roland, C. M.; Hensel-Bielowka, S.; Paluch, M.; Casalini, R. Supercooled dynamics of glass-forming liquids and polymers under hydrostatic pressure. *Rep. Prog. Phys.* **2005**, *68*, 1405−1478.
(26) Casalini, R.; Roland, C. M. Pressure evolution of the excess wing in a type-B glass former. *Phys. Rev. Lett.* **2003**, *91*, 015702.
(27) Tu, W.; Valenti, S.; Ngai, K. L.; Capaccioli, S.; Liu, Y. D.; Wang, L.-M. Direct Evidence of Relaxation Anisotropy Resolved by High Pressure in a Rigid and Planar Glass Former. *J. Phys. Chem. Lett.* **2017**, *8*, 4341−4346.
(28) Casalini, R.; Snow, A. W.; Roland, C. M. Temperature Dependence of the Johari−Goldstein Relaxation in Poly(methyl methacrylate) and Poly(thiomethyl methacrylate). *Macromolecules* **2013**, *46*, 330−334.
(29) Yu, H.-B.; Richert, R.; Samwer, K. Structural rearrangements governing Johari-Goldstein relaxations in metallic glasses. *Sci. Adv.* **2017**, *3*, e1701577.
(30) Stevenson, J. D.; Wolynes, P. G. A universal origin for secondary relaxations in supercooled liquids and structural glasses. *Nat. Phys.* **2010**, *6*, 62.
(31) Tanaka, H. Origin of the excess wing and slow β relaxation of glass formers: A unified picture of local orientational fluctuations. *Phys. Rev. E* **2004**, *69*, 021502.
(32) Fragiadakis, D.; Roland, C. M. Characteristics of the Johari-Goldstein process in rigid asymmetric molecules. *Phys. Rev. E* **2013**, *88*, 042307.
(33) Zhu, F.; Nguyen, H. K.; Song, S. X.; Aji, D. P. B.; Hirata, A.; Wang, H.; Nakajima, K.; Chen, M. W. Intrinsic correlation between beta-relaxation and spatial heterogeneity in a metallic glass. *Nat. Commun.* **2016**, *7*, 11516.
(34) Liu, Y. H.; Fujita, T.; Aji, D. P. B.; Matsuura, M.; Chen, M. W. Structural origins of Johari-Goldstein relaxation in a metallic glass. *Nat. Commun.* **2014**, *5*, 3238.
(35) Fragiadakis, D.; Roland, C. M. Role of structure in the alpha and beta dynamics of a simple glass-forming liquid. *Phys. Rev. E* **2017**, *95*, 022607.
(36) Cohen, Y.; Karmakar, S.; Procaccia, I.; Samwer, K. The nature of the beta-peak in the loss modulus of amorphous solids. *Europhys. Lett.* **2012**, *100*, 36003.
(37) Yu, H. B.; Wang, W. H.; Bai, H. Y.; Wu, Y.; Chen, M. W. Relating activation of shear transformation zones to β relaxations in metallic glasses. *Phys. Rev. B* **2010**, *81*, 220201.
(38) Yu, H. B.; Shen, X.; Wang, Z.; Gu, L.; Wang, W. H.; Bai, H. Y. Tensile plasticity in metallic glasses with pronounced beta relaxations. *Phys. Rev. Lett.* **2012**, *108*, 015504.
(39) Wang, Z.; Sun, B. A.; Bai, H. Y.; Wang, W. H. Evolution of hidden localized flow during glass-to-liquid transition in metallic glass. *Nat. Commun.* **2014**, *5*, 5823.
(40) Xiao, C.; Jho, J. Y.; Yee, A. F. Correlation between the Shear Yielding Behavior and Secondary Relaxations of Bisphenol A Polycarbonate and Related Copolymers. *Macromolecules* **1994**, *27*, 2761−2768.
(41) Kissi, E. O.; Grohganz, H.; Lobmann, K.; Ruggiero, M. T.; Zeitler, J. A.; Rades, T. Glass-Transition Temperature of the beta-Relaxation as the Major Predictive Parameter for Recrystallization of Neat Amorphous Drugs. *J. Phys. Chem. B* **2018**, *122*, 2803−2808.
(42) Ngai, K. L.; Capaccioli, S.; Prevosto, D.; Wang, L.-M. Coupling of Caged Molecule Dynamics to JG beta-Relaxation II: Polymers. *J. Phys. Chem. B* **2015**, *119*, 12502−12518.
(43) Sun, Y.; Concustell, A.; Greer, A. L. Thermomechanical processing of metallic glasses: extending the range of the glassy state. *Nat. Rev. Mater.* **2016**, *1*, 16039.
(44) Donati, C.; Douglas, J. F.; Kob, W.; Plimpton, S. J.; Poole, P. H.; Glotzer, S. C. Stringlike Cooperative Motion in a Supercooled Liquid. *Phys. Rev. Lett.* **1998**, *80*, 2338−2341.

DOI: 10.1021/acs.jpclett.8b02629
J. Phys. Chem. Lett. 2018, 9, 5877−5883

(45) Zhang, H.; Srolovitz, D. J.; Douglas, J. F.; Warren, J. A. Grain Boundaries Exhibit the Dynamics of Glass-Forming Liquids. *Proc. Natl. Acad. Sci. U. S. A.* **2009**, *106*, 7735−7740.
(46) Starr, F.; Douglas, J.; Sastry, S. The Relationship of Dynamical Heterogeneity to the Adam-Gibbs and Random First-Order Transition Theories of Glass Formation. *J. Chem. Phys.* **2013**, *138*, 12A541.
(47) Zhang, H.; Zhong, C.; Douglas, J. F.; Wang, X.; Cao, Q.; Zhang, D.; Jiang, J.-Z. Role of string-like collective atomic motion on diffusion and structural relaxation in glass forming Cu-Zr alloys. *J. Chem. Phys.* **2015**, *142*, 164506.
(48) Lam, C.-H. Repetition and pair-interaction of string-like hopping motions in glassy polymers. *J. Chem. Phys.* **2017**, *146*, 244906.
(49) Yu, H. B.; Richert, R.; Maaß, R.; Samwer, K. Unified Criterion for Temperature-Induced and Strain-Driven Glass Transitions in Metallic Glass. *Phys. Rev. Lett.* **2015**, *115*, 135701.
(50) Johari, G. P. Glass transition and secondary relaxations in molecular liquids and crystals. *Ann. N. Y. Acad. Sci.* **1976**, *279*, 117−140.
(51) Capaccioli, S.; Ngai, K. L.; Thayyil, M. S.; Prevosto, D. Coupling of Caged Molecule Dynamics to JG beta-Relaxation: I. *J. Phys. Chem. B* **2015**, *119*, 8800−8808.
(52) Ngai, K. L.; Capaccioli, S.; Prevosto, D.; Wang, L.-M. Coupling of Caged Molecule Dynamics to JG beta-Relaxation III: van der Waals Glasses. *J. Phys. Chem. B* **2015**, *119*, 12519−12525.
(53) Wang, Z.; Ngai, K. L.; Wang, W. H.; Capaccioli, S. Coupling of caged molecule dynamics to Johari-Goldstein beta-relaxation in metallic glasses. *J. Appl. Phys.* **2016**, *119*, 024902.
(54) Paluch, M.; Knapik, J.; Wojnarowska, Z.; Grzybowski, A.; Ngai, K. L. Universal Behavior of Dielectric Responses of Glass Formers: Role of Dipole-Dipole Interactions. *Phys. Rev. Lett.* **2016**, *116*, 025702.
(55) Vogel, M.; Glotzer, S. C. Spatially Heterogeneous Dynamics and Dynamic Facilitation in a Model of Viscous Silica. *Phys. Rev. Lett.* **2004**, *92*, 255901.
(56) Sheng, H. W.; Luo, W. K.; Alamgir, F. M.; Bai, J. M.; Ma, E. Atomic packing and short-to-medium-range order in metallic glasses. *Nature* **2006**, *439*, 419−425.
(57) Sheng, H. W.; Ma, E.; Kramer, M. J. Relating Dynamic Properties to Atomic Structure in Metallic Glasses. *JOM* **2012**, *64*, 856−881.
(58) Wang, Q.; Li, J. H.; Liu, J. B.; Liu, B. X. Favored Composition Design and Atomic Structure Characterization for Ternary Al−Cu−Y Metallic Glasses via Proposed Interatomic Potential. *J. Phys. Chem. B* **2014**, *118*, 4442−4449.
(59) Yu, H.-B.; Samwer, K. Atomic mechanism of internal friction in a model metallic glass. *Phys. Rev. B* **2014**, *90*, 144201.
(60) Yu, H.-B.; Richert, R.; Samwer, K. Correlation between Viscoelastic Moduli and Atomic Rearrangements in Metallic Glasses. *J. Phys. Chem. Lett.* **2016**, *7*, 3747−3751.

DOI: 10.1021/acs.jpclett.8b02629
J. Phys. Chem. Lett. 2018, 9, 5877−5883